Low-Temperature Synthesis of Large-Scale Molybdenum Disulfide Thin Films Directly on a Plastic Substrate Using Plasma-Enhanced Chemical Vapor Deposition

Chisung Ahn, Jinhwan Lee, Hyeong-U Kim, Hunyoung Bark, Minhwan Jeon, Gyeong Hee Ryu, Zonghoon Lee, Geun Young Yeom, Kwangsu Kim, Jaehyuck Jung, Youngseok Kim, Changgu Lee, and Taesung Kim**

Transition metal dichalcogenides (TMDs) that form layered structures have many applications due to their excellent electrical,[1] mechanical,[2] and optical[3] properties. Among the TMDs, molybdenum disulfide (MoS_2) has attracted particular interest because it has a bandgap that can be tuned from an indirect bandgap of 1.29 eV in its bulk form to a direct bandgap of 1.90 eV as a monolayer.[4] Mechanical exfoliation using adhesive tape is a typical method employed to synthesize MoS_2 consisting of a few layers. This method yields a highly crystalline MoS_2 product with pristine quality because the product is directly extracted from a bulk MoS_2 crystal. However, the yield of this exfoliation method is very low and the resulting product is small, ranging from a few micrometers to a few tens of micrometers,[4,5] which limits large-scale applications. Meanwhile, syntheses of various kinds of large 2D materials, especially TMDs, by using thermal chemical vapor deposition (thermal-CVD),[6] have been pursued based on the thermal decomposition of feedstock.[7,8] Even though thermal-CVD methods have various advantages for the synthesis of nanomaterials, such as conformal coverage, selective deposition, and mass production, they have critical limitations in the direct synthesis on plastic substrates for flexible transparent device applications because of the relatively high (>600 °C) processing temperatures used, which are two to three times higher than the glass transition temperatures of most plastic substrates.[9] Due to such challenges, in practice large-area films made of 2D materials are thermally synthesized on hard substrates, such as SiO_2, quartz, and metals, and then transferred onto plastic substrates for flexible device fabrication. However, the transfer process results in imperfect contacts, cracks, defects, and contamination, which degrade the device performance significantly.[10] Therefore, to achieve large-scale synthesis of high-quality MoS_2 thin films using temperatures lower than the glass transition temperature of the plastic substrate, innovative methods for synthesizing 2D thin films need to be developed.

To overcome the limitations of previous MoS_2 thin film synthesis methods, plasma-enhanced CVD (PECVD) has been introduced to effectively dissociate feedstock gases by cold plasma generation in this work. Compared with thermal-CVD methods, PECVD offers the advantages of relatively low substrate temperature, better control of nanostructure formation and uniform thickness due to the presence of accelerated energetic electrons, excited molecules and atoms, free radicals, photons, and other active species in the plasma.[11] Also, since the reactive and energetic species in the gas phase are formed by collisions in the plasma above the substrate, the substrate can be maintained at a low temperature. Hence, the overall synthesis temperature of PECVD is lower than that of the conventional thermal-CVD process. Due to these advantages, many kinds of semiconducting materials as well as insulating materials have been synthesized and broadly used in industry.[12,13] As a representative example, the synthesis of thin film graphene using PECVD under a relatively low temperature of 400 °C was recently reported.[14]

In the present study, the direct synthesis of layered MoS_2 thin films on a large-area polyimide (PI) substrate was achieved at a substrate temperature as low as 150 °C using a Mo sulfurization mechanism in an inductively coupled plasma (ICP) system. Our work demonstrates the promise of MoS_2 thin film synthesis directly on a flexible plastic substrate without a transfer process, when cold plasma is used to dissociate H_2S gas. Normally, most other types of thin films synthesized using PECVD are deposited by the adsorption and reaction of precursors on the substrate surface after the dissociation of feedstock gases and gas-phase reaction for making the precursors.[12,14,15] In this study, however, Mo metal was deposited on the PI substrate as a precursor and sulfurized by the dissociated H_2S

C. Ahn, H. Kim, H. Bark, M. Jeon, G. Y. Yeom, J. Jung, Prof. C. Lee, Prof. T. Kim
SKKU Advanced Institute of Nanotechnology (SAINT)
Sungkyunkwan University
2066 Seobu-ro, Jangan-gu, Suwon, Gyeonggi-do 440-746, South Korea
E-mail: peterlee@skku.edu; tkim@skku.edu

J. Lee, Y. Kim, C. Lee, T. Kim
School of Mechanical Engineering
Sungkyunkwan University
2066 Seobu-ro, Jangan-gu, Suwon, Gyeonggi-do 440-746, South Korea
G. H. Ryu, Z. Lee
School of Materials Science and Engineering
Ulsan National Institute of Science and Technology (UNIST)
50 UNIST-gil, Eonyang-eup, Ulsan 689-798, South Korea
G. Y. Yeom
School of Advanced Materials Science & Engineering
Sungkyunkwan University
2066 Seobu-ro, Jangan-gu, Suwon, Gyeonggi-do 440-746, South Korea
K. Kim
Semiconductor R&D Center
Samsung Electronics
1 Samsungjeonja-ro, Hwaseong, Gyeonggi-do 445-701, South Korea

DOI: 10.1002/adma.201501678

© 2015 WILEY-VCH Verlag GmbH & Co. KGaA, Weinheim

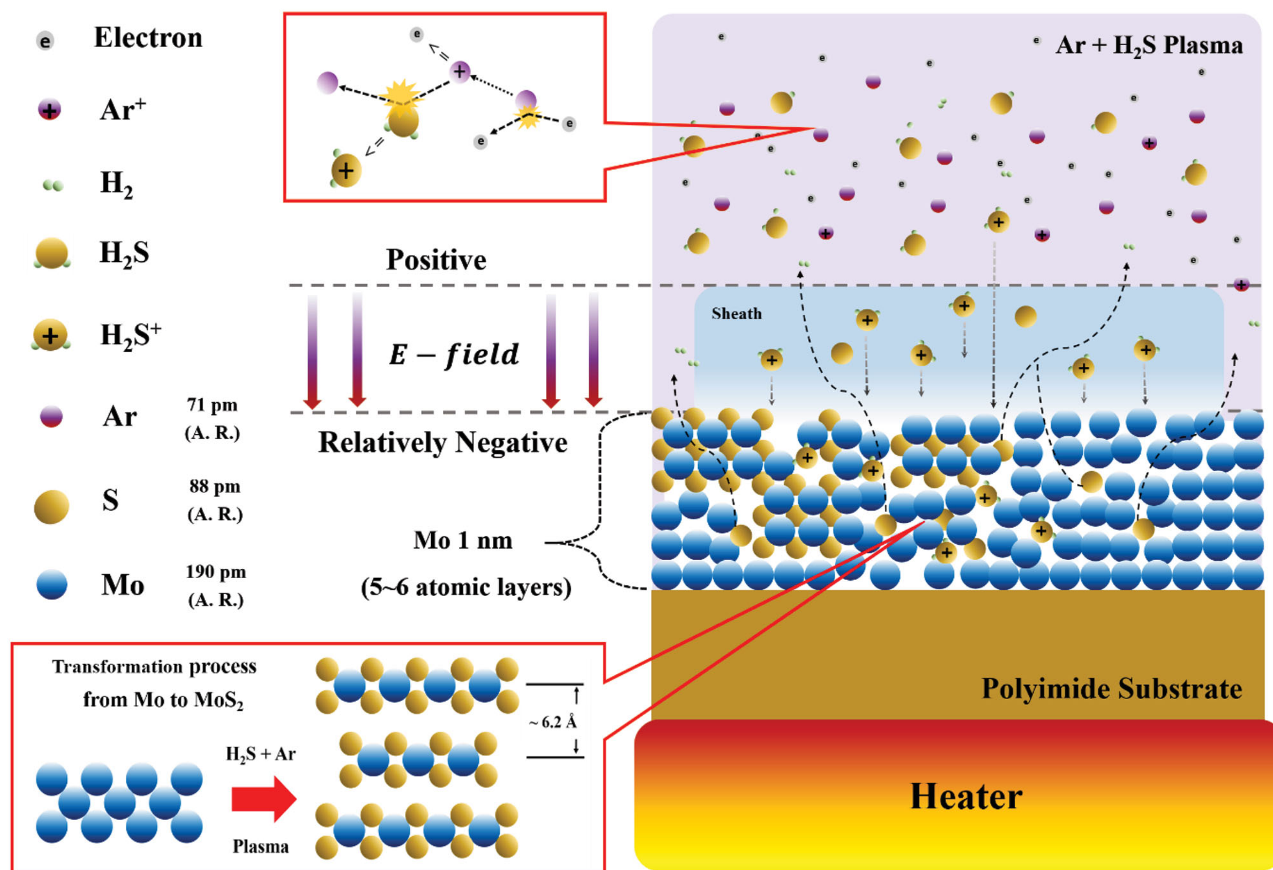

Figure 1. The mechanism for the synthesis of a thin-layered MoS_2 thin film by PECVD.

gas to synthesize the MoS_2 thin film. This approach may be explained by the following hypothetical mechanism that is shown in **Figure 1**: i) ionization of argon (Ar) gas,[16] leading to a charge transfer reaction and the generation of H_2S ions (top inset of Figure 1); ii) transport and implantation of H_2S ions as a sheath layer on the Mo metal layer, driven by an electric field; and iii) sulfurization of Mo by the H_2S ions with formation of hydrogen (H_2) gas as a byproduct. Meanwhile, the atomic radius of Mo is about 1.9 Å[17] and 1 nm of Mo metal film corresponds to five to six layers of Mo atoms. Once this Mo film is fully sulfurized to MoS_2 thin film, its thickness should be five to six layers of about 4 nm following the transformation process as shown in the bottom inset of Figure 1. The characterization of synthesized MoS_2 thin films by the mentioned hypothesis will be discussed later.

A photograph of a PI substrate (half-covered) with the MoS_2 thin film that was synthesized using Ar + H_2S plasma and the synthesis procedures are shown in **Figure 2**. Raman spectra of the MoS_2 thin films synthesized at 150 and 300 °C (**Figure 3**a) were both observed to contain the E^1_{2g} and A_{1g} modes of in-plane and out-of-plane vibrations that are typical for MoS_2 crystals; the distance between the peaks was observed to be

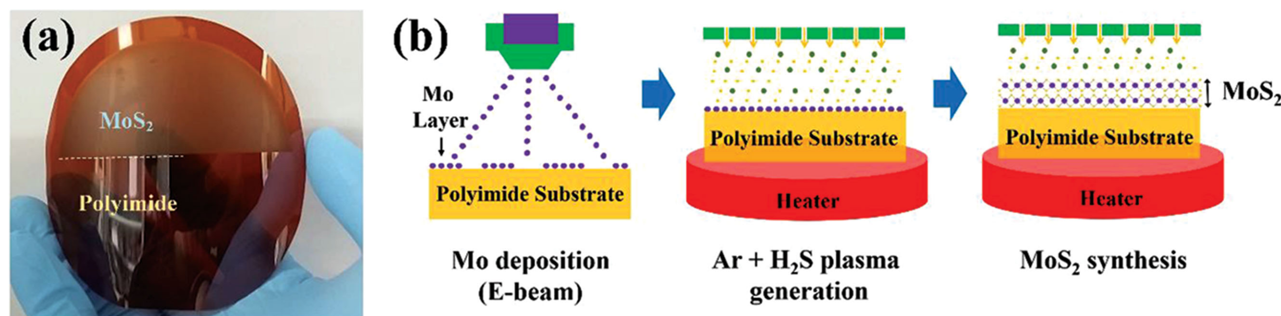

Figure 2. Wafer-scale synthesis of MoS_2 thin films by PECVD. a) Image of the MoS_2 thin film deposited on half of the surface of a 4 in. wafer-scale PI substrate to clearly visualize. b) Schematic illustration of the direct synthesis process.

© 2015 WILEY-VCH Verlag GmbH & Co. KGaA, Weinheim

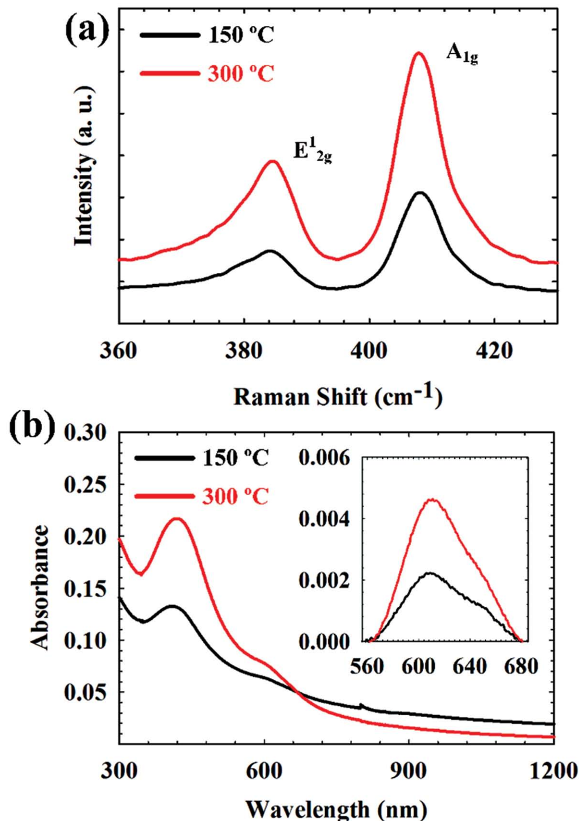

Figure 3. Optical properties of the MoS_2 thin films synthesized at 150 and 300 °C on the PI substrate. a) Raman spectra of the $E^1{}_{2g}$ and A_{1g} modes. b) UV–vis absorbance spectra. Inset: normalized spectra from 560 to 680 nm.

24 cm^{-1}, suggestive of five to six layers of MoS_2 in the thin film with a thickness of 3–4 nm.[18] The Raman spectra on various positions of 4 in. wafer scale had confirmed the uniformity of MoS_2 thin film thickness by repetitive intensities and distance between $E^1{}_{2g}$ and A_{1g} (Figure S1, Supporting Information). The UV–vis absorption spectra of these two films (Figure 3b) were also collected, in order to characterize their optical properties. These spectra revealed four peaks corresponding to the optical transitions between d-orbitals in the visible range from 390 to 700 nm.[19] The A and B peaks, located at 651 (1.91 eV) and 610 nm (2.04 eV), respectively, are related to the direct bandgaps situated at the K point of the Brillouin zone[20] and are consistent with reported optical absorption data.[20]

The binding energy and atomic ratio of the synthesized MoS_2 thin films were checked using X-ray photoelectron spectroscopy (XPS), as shown in **Figure 4** and Table S2 (Supporting Information). The 2H-MoS_2 thin film synthesized at 150 °C on the PI substrate (Figure 4a) yielded Mo binding energies of 229.6 and 232.7 eV, which correspond to Mo $3d_{5/2}$ and Mo $3d_{3/2}$, respectively, and S binding energies of 162.5 and 163.7 eV, corresponding to S $2p_{3/2}$ and S $2p_{1/2}$, respectively,[21] with a 1:1.87 atomic ratio of Mo to S. The small difference between this relative amount of S and the stoichiometrically expected value of 2 may be due to the small peak near 236 eV corresponding to Mo $^{6+}$ ligands,[22] which may have resulted from oxidation of the MoS_2 thin film. Normally, sulfur vacancies in transition metal disulfides are active sites for oxygen chemisorption.[23] The relatively low processing temperature apparently negatively affected the crystallinity of the synthesized MoS_2 thin films through the formation of a small quantity of oxide in the vacancy sites. Another sample synthesized at 300 °C (Figure 4b) showed a 1:1.95 atomic ratio of Mo to S, and the same binding energies of Mo and S atoms as in the 150 °C processing condition. The improved stoichiometry at 300 °C indicates that, at this temperature, less oxide formed and the films were produced with a higher crystalline quality than when the films were made at 150 °C, suggesting that an increased temperature improves the quality of the synthesized film.

High-resolution transmission electron microscopy (HR-TEM) was used to characterize the thickness and crystallinity of the MoS_2 thin films synthesized at 150 and 300 °C, as shown in **Figure 5**a–d. According to this analysis, the MoS_2 thin films synthesized at these temperatures consisted of a few layers, consistent with the Raman spectroscopy results. The films synthesized at 150 and 300 °C showed a polycrystalline structure with average domain sizes of 5 and 7 nm, respectively. This observation also suggests a better quality for the film grown at the higher temperature. The domain size in the films depended on the mass of H_2S ions diffused to and deposited on Mo, driven by the electrical field in the sheath region, and on the degree of sulfurization resulting from thermal-dependent parameters. The morphology and thickness of the MoS_2 thin films were also investigated using atomic force microscopy (AFM). The thickness of the film grown at 150 °C and that at 300 °C were observed by AFM to be 3.75 and 3.88 nm, respectively (Figure 5e,f), which are similar to the values obtained from the TEM analysis. Moreover, when initial thickness of Mo metal was smaller than 1 nm, thickness of MoS_2 thin film decreased with the linear proportion (Figure S2, Supporting Information).

To characterize the electrical properties of the MoS_2 thin films synthesized on PI substrate, Hall measurements were carried out at various positions on the 4 in. substrate using the van der Pauw method.[24] The mobility was derived from these Hall measurements from 50 points over the 4 in. PI substrates as shown in **Figure 6**. The average mobilities and charge concentrations of the MoS_2 thin films grown at 150 and 300 °C were determined to be 2.014 and 3.710 $cm^2 V^{-1} s^{-1}$, respectively. The corresponding average charge densities were -2.13×10^{19} and -5.16×10^{17} cm^{-3} (see Table S1 for specific numbers, Supporting Information). All the MoS_2 thin films showed negative charge concentration values resulting from contained electrons as the main charge carrier, which means that the MoS_2 thin films acted as n-type semiconductors, as expected for typical MoS_2 crystals.

As an application, MoS_2 thin-film-based flexible humidity sensors were fabricated using the MoS_2 film grown on a PI substrate at 300 °C. From the I_{DS}–V_{DS} characteristics for different relative humidity (RH) from 15% to 95%, we could observe the gradual decrease of gradients with increase in RH as shown in **Figure 7**a. Also, the resistance change as a function of RH was confirmed from the I_{DS}–V_{DS} results, which is compatible with the

© 2015 WILEY-VCH Verlag GmbH & Co. KGaA, Weinheim

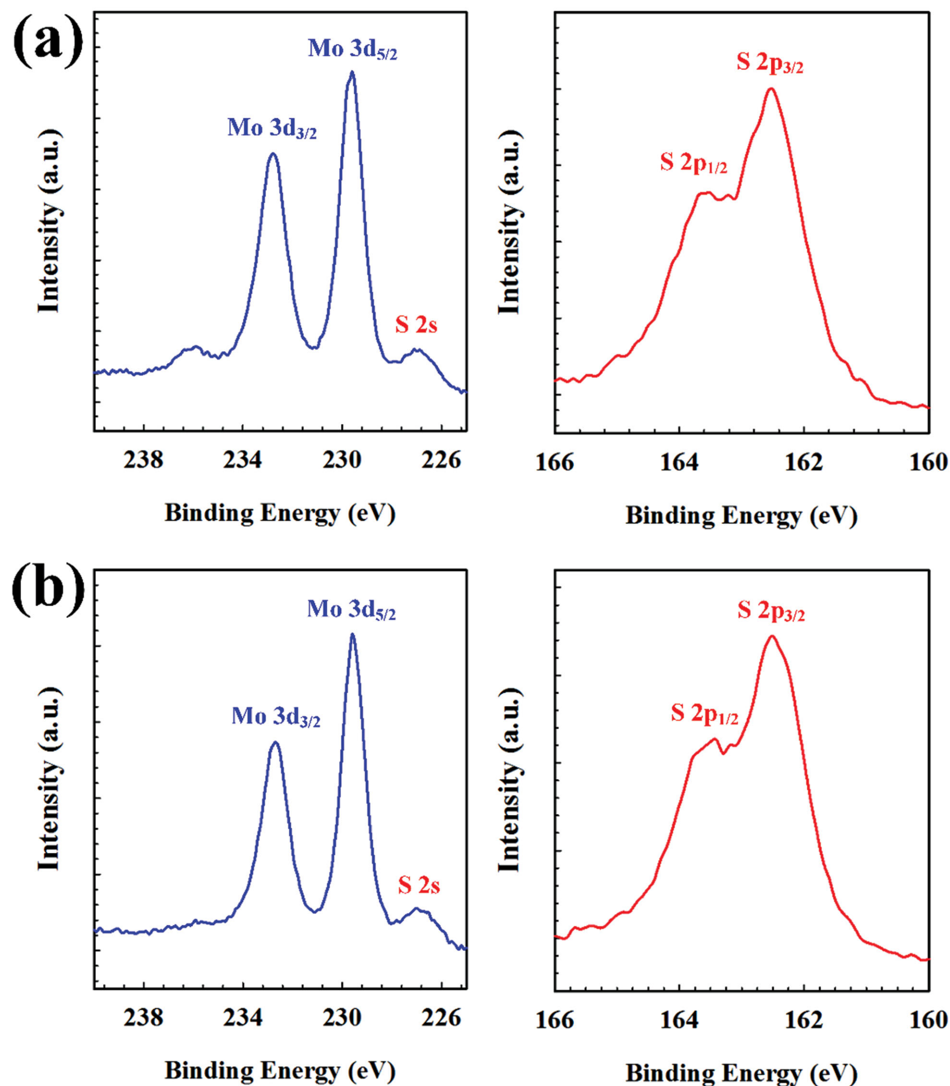

Figure 4. X-ray photoluminescence spectroscopy (XPS) analyses of MoS_2 thin films synthesized on PI substrates at processing temperatures of a) 150 and b) 300 °C.

previous reports.[25] The inset of Figure 7b shows the MoS_2 flexible humidity sensor arrays on PI substrate with a size of 5 cm^2.

During the formation of films using PECVD, the argon gas plasma and a high plasma power typically cause surface defects to develop on the synthesized materials,[26] and such defects can play a role in limiting the quality of the synthesized thin films.[27] An increased ratio of Ar to H_2S gas indeed resulted in a decrease of the Raman intensities in the synthesized MoS_2 thin film samples with other sulfurization conditions fixed (data not shown). Therefore, more detailed investigations are planned that aim to modify the properties of PECVD-synthesized MoS_2 thin films by varying the gas ratio and plasma power, and these studies will also include measurements for deriving information about the radicals produced.

In conclusion, we have demonstrated the growth of MoS_2 thin films directly on PI substrates by the sulfurization of Mo at 150 °C and that at 300 °C substrate temperatures in an ICP system. At these low temperatures, the MoS_2 crystal formed well, without any thermal damage to the plastic substrate. To the best of our knowledge, these are the lowest temperatures ever reported for a CVD synthesis of a metal chalcogenide crystal yielding large, uniform, and continuous films on the scale of several inches. Also, it is the first report of the direct deposition of a 2D crystal on a soft substrate without using a transfer method, which causes many structural defects. The carrier mobility of ≈3.7 $cm^2\ V^{-1}\ s^{-1}$ derived from the Hall measurement reveals that these films have a structural integrity good enough to be used for electronic devices. In addition, the successful detection of humidity by the MoS_2 thin film synthesized on PI substrate reveals its potential for flexible sensor devices. Our approach and results open a new way for the synthesis of 2D crystals directly on soft substrates at low temperatures, and should be of use for the fabrication of transparent flexible semiconductor devices with high quality and uniformity.

© 2015 WILEY-VCH Verlag GmbH & Co. KGaA, Weinheim

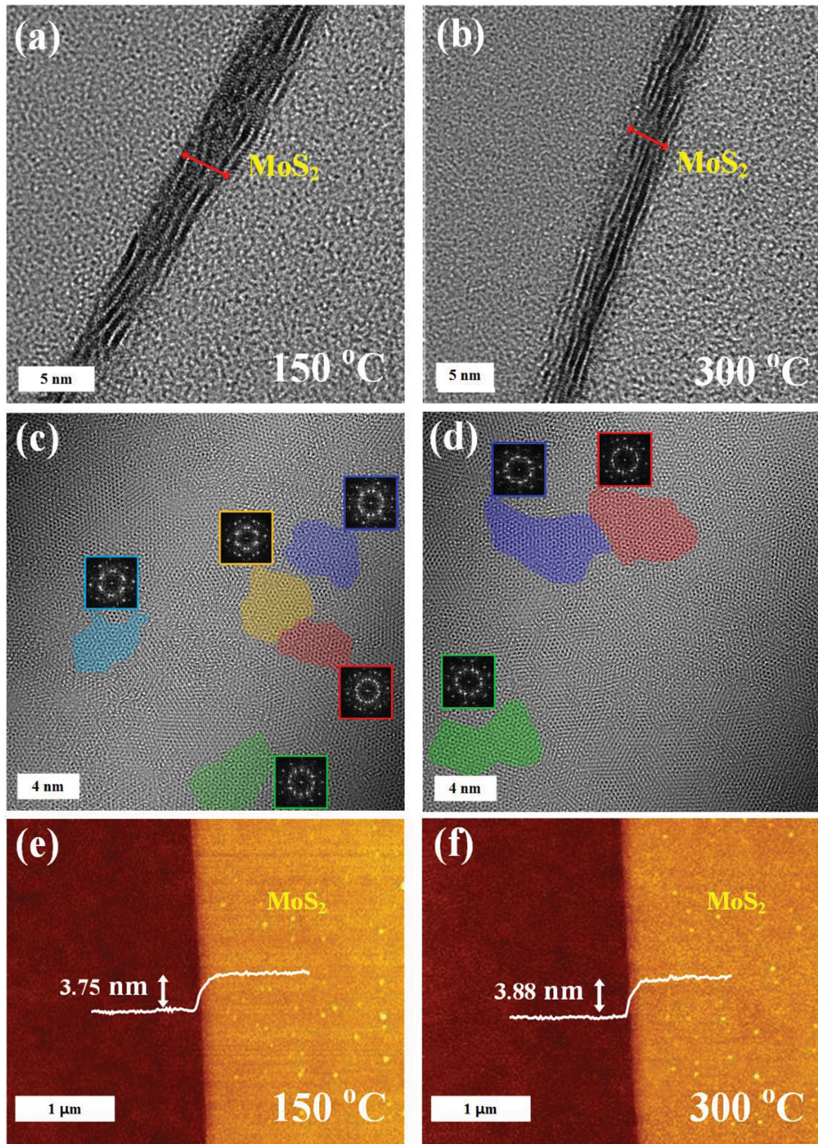

Figure 5. Structural properties from microscopy images of the MoS_2 thin films synthesized at a,c,e) 150 and b, d, f) 300 °C. High-resolution transmission electron microscopy (HR-TEM) images of the synthesized MoS_2 thin films, along with a,b) cross-sectional views and c,d) grain size analysis. e,f) Topological images and line profiles by atomic force microscopy (AFM).

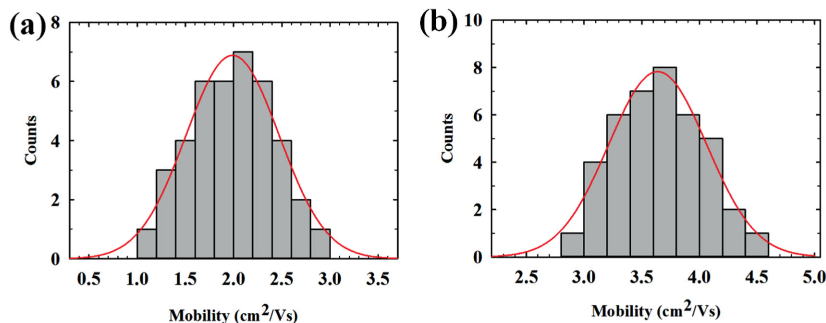

Figure 6. Hall mobility histograms of MoS_2 thin films synthesized on PI substrates at a) 150 and b) 300 °C obtained from 40 points on the substrates.

Experimental Section

Synthesis: In order to evaluate the feasibility of synthesizing layered MoS_2 thin films using PECVD, a 1 nm thick layer of Mo was initially deposited on a 4 in. PI wafer substrate by an e-beam evaporator,[8] followed by sulfurization using the PECVD system under inert Ar plasma conditions. Ar-generated plasma decomposed the H_2S gas to produce the sulfur precursor, leading to the synthesis of layered MoS_2 thin films through sulfurization of Mo. To obtain high-quality MoS_2 thin films, vacuum conditions under 10^{-5} Torr were used after loading Mo-deposited PI substrate in the PECVD system, while venting the system with Ar gas for generating inert conditions and removing any residue contamination. For the next step, Mo-deposited PI substrate was treated with H_2 gas plasma because it can remove native oxide film on the substrate without other contamination effects. After thermally activating the substrate by elevating its temperature in an inert Ar atmosphere, H_2S and Ar gases were introduced into the PECVD system and the plasma was generated by controlling conditions such as chamber pressure, plasma power, and flow rate of gases. All the synthesis steps and process conditions for characterization of layered MoS_2 thin films are illustrated in Figure S3 and Table S3, respectively (Supporting Information).

Characterization of MoS_2: Synthesized MoS_2 thin films were analyzed by Raman spectroscopy, UV–vis spectroscopy, XPS, and TEM. A laser with a wavelength of 532 nm operating at 2 mW was used in the Raman study. The MoS_2 thin films were synthesized on a transparent quartz substrate for the analysis of UV–vis absorbance (Cary 5000 UV–vis–NIR, Agilent Technologies). The binding energies and atomic compositions of the MoS_2 thin films were confirmed by using an X-ray photoelectron spectrometer (ESCA2000, VG Microtech Inc.) with an Mg Kα X-ray. The atomic structure and thickness of each film were verified using HR-TEM (Titan, FEI). These films were transferred onto a TEM grid using the conventional wet transfer method for the top view and the focused ion beam process for viewing the cross sections. Moreover, the thickness of each film was confirmed by AFM (E-Sweep, Seiko Instruments Inc.).

Processing temperatures of 300 and 150 °C were selected in order to show potential applications of direct MoS_2 thin film synthesis on various types of flexible plastic substrates. It is well known that the glass transition temperature (deformation temperature) of PI is >300 °C and that of poly(ethylene naphthalate) (PEN) is 155 °C;[28] hence, in the present study the direct synthesis of MoS_2 thin films on PI substrates for the above-mentioned temperatures was evaluated.

MoS_2-Based Flexible Humidity Sensor: The sensor devices were fabricated using e-beam evaporator for deposition of Au electrode on MoS_2 thin film having a channel length of 100 μm and a width of 1000 μm. For the humidity detection, humidity was maintained by controlling the evaporation amount of water in the homemade isolated chamber with an installed hygrometer, which was connected to 2 probe tip outward. The I_{DS}–V_{DS} curve was measured by Keithley 4200-SCS

© 2015 WILEY-VCH Verlag GmbH & Co. KGaA, Weinheim

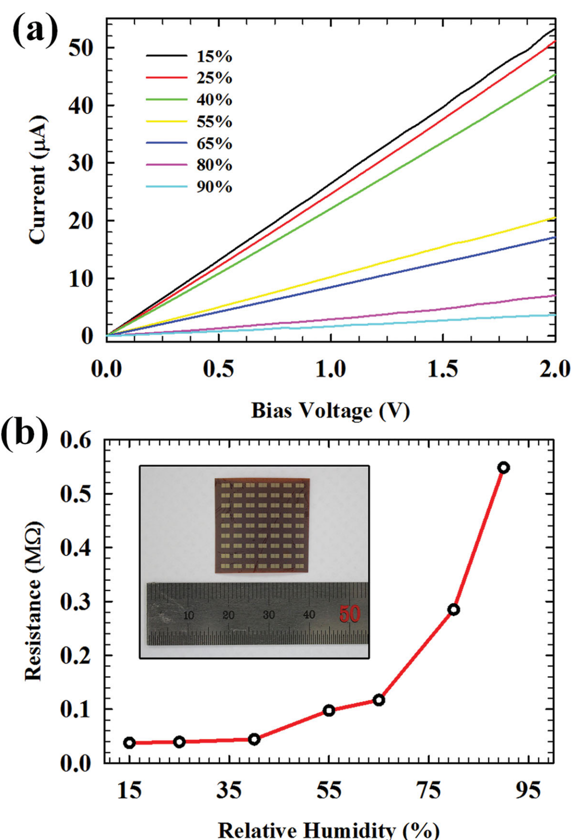

Figure 7. Characterization of humidity detection on a MoS_2 thin film synthesized on PI substrate a) I_{DS}–V_{DS} characteristic and b) resistance behavior toward different RH from 15% to 95%. The inset of (b) shows the MoS_2 flexible humidity sensor arrays on PI substrate and a ruler (millimeter units) for size comparison.

semiconductor characterization system on real time toward applied bias voltage from 0 to 2 V and the resistances were calculated for each RH.

Supporting Information

Supporting Information is available from the Wiley Online Library or from the author.

Acknowledgements

C.A. and J.L. contributed equally to this work. This study was supported by National Research Foundation of Korea (NRF) grants funded by the Korean Government Ministry of Science, ICT and Future Planning (MSIP) (No. 2009-0083540), by the Center for Advanced Soft-Electronics funded by the Ministry of Science, ICT and Future Planning (MSIP) as Global Frontier Project (2011-0031630), and by the Global Frontier R&D Program on Center for Multiscale Energy System funded by the National Research Foundation under the Ministry of Science, ICT and Future Planning, Korea (NRF-2012M3A6A7054863).

Note: The unit scale on the ruler in the caption of Figure 7 was corrected to millimeters on September 10, 2015, after initial publication online.

Received: April 9, 2015
Revised: June 22, 2015
Published online: August 10, 2015

[1] S. Ghatak, A. N. Pal, A. Ghosh, *ACS Nano* **2011**, *5*, 7707.
[2] A. Castellanos-Gomez, M. Poot, G. A. Steele, H. S. J. van der Zant, N. Agrait, G. Rubio-Bollinger, *Nanoscale Res. Lett.* **2012**, *7*, 1.
[3] a) Z. Y. Yin, H. Li, H. Li, L. Jiang, Y. M. Shi, Y. H. Sun, G. Lu, Q. Zhang, X. D. Chen, H. Zhang, *ACS Nano* **2012**, *6*, 74; b) O. Lopez-Sanchez, D. Lembke, M. Kayci, A. Radenovic, A. Kis, *Nat. Nanotechnol.* **2013**, *8*, 497.
[4] K. F. Mak, C. Lee, J. Hone, J. Shan, T. F. Heinz, *Phys. Rev. Lett.* **2010**, *105*, 136805.
[5] a) A. Splendiani, L. Sun, Y. B. Zhang, T. S. Li, J. Kim, C. Y. Chim, G. Galli, F. Wang, *Nano Lett.* **2010**, *10*, 1271; b) J. Brivio, D. T. L. Alexander, A. Kis, *Nano Lett.* **2011**, *11*, 5148.
[6] a) X. S. Li, C. W. Magnuson, A. Venugopal, R. M. Tromp, J. B. Hannon, E. M. Vogel, L. Colombo, R. S. Ruoff, *J. Am. Chem. Soc.* **2011**, *133*, 2816; b) S. Lee, K. Lee, Z. H. Zhong, *Nano Lett.* **2010**, *10*, 4702.
[7] a) N. Choudhary, J. Park, J. Y. Hwang, W. Choi, *ACS Appl. Mater. Interfaces* **2014**, *6*, 21215; b) J. Xia, X. Huang, L. Z. Liu, M. Wang, L. Wang, B. Huang, D. D. Zhu, J. J. Li, C. Z. Gu, X. M. Meng, *Nanoscale* **2014**, *6*, 8949; c) Y. H. Lee, X. Q. Zhang, W. J. Zhang, M. T. Chang, C. T. Lin, K. D. Chang, Y. C. Yu, J. T. W. Wang, C. S. Chang, L. J. Li, T. W. Lin, *Adv. Mater.* **2012**, *24*, 2320; d) C. Cong, J. Shang, X. Wu, B. Cao, N. Peimyoo, C. Qiu, L. Sun, T. Yu, *Adv. Optical Mater.* **2014**, *2*, 131.
[8] a) Y. J. Zhan, Z. Liu, S. Najmaei, P. M. Ajayan, J. Lou, *Small* **2012**, *8*, 966; b) Y. Lee, J. Lee, H. Bark, I. K. Oh, G. H. Ryu, Z. Lee, H. Kim, J. H. Cho, J. H. Ahn, C. Lee, *Nanoscale* **2014**, *6*, 2821.
[9] a) E. L. Bedia, S. Murakami, T. Kitade, S. Kohjiya, *Polymer* **2001**, *42*, 7299; b) Z. Peng, L. Yu, *Macromolecules* **1994**, *27*, 2638.
[10] a) Y. F. Zhang, T. Gao, Y. B. Gao, S. B. Xie, Q. Q. Ji, K. Yan, H. L. Peng, Z. F. Liu, *ACS Nano* **2011**, *5*, 4014; b) X. L. Liang, B. A. Sperling, I. Calizo, G. J. Cheng, C. A. Hacker, Q. Zhang, Y. Obeng, K. Yan, H. L. Peng, Q. L. Li, X. X. Zhu, H. Yuan, A. R. H. Walker, Z. F. Liu, L. M. Peng, C. A. Richter, *ACS Nano* **2011**, *5*, 9144.
[11] a) D. Flamm, in *Plasma Processing of Semiconductors, NATO ASI Series, Series E: Applied Sciences, Vol. 336*, (Ed: P. F. Williams), Kluwer Academic Publishers, Dordrecht, The Netherlands/Boston, MA, USA/London, UK **1997**, p. 23; b) A. Grill, *Cold Plasma in Materials Fabrication: From Fundamentals to Applications*, IEEE, New York, **1994**.
[12] a) A. Barranco, J. Cotrino, F. Yubero, J. P. Espinos, J. Benitez, C. Clerc, A. R. Gonzalez-Elipe, *Thin Solid Films* **2001**, *401*, 150; b) A. Sazonov, D. Striakhilev, C. H. Lee, A. Nathan, *Proc. IEEE* **2005**, *93*, 1420.
[13] W. G. Lee, S. I. Woo, J. C. Kim, S. H. Choi, K. H. Oh, *Thin Solid Films* **1994**, *237*, 105.
[14] Z. Bo, Y. Yang, J. H. Chen, K. H. Yu, J. H. Yan, K. F. Cen, *Nanoscale* **2013**, *5*, 5180.
[15] Z. P. Wang, M. Shoji, H. Ogata, *Appl. Surf. Sci.* **2011**, *257*, 9082.
[16] a) K. Gutsol, T. Nunnally, A. Rabinovich, A. Fridman, A. Starikovskiy, A. Gutsol, A. Kemoun, *Int. J. Hydrogen Energy* **2012**, *37*, 1335; b) E. L. Reddy, V. M. Biju, C. Subrahmanyam, *Appl. Energy* **2012**, *95*, 87.
[17] B. Averill, P. Eldredge, *General Chemistry: Principles, Patterns, and Applications*, Saylor Foundation, Washington, D.C. **2011**.
[18] C. Lee, H. Yan, L. E. Brus, T. F. Heinz, J. Hone, S. Ryu, *ACS Nano* **2010**, *4*, 2695.
[19] a) L. F. Mattheiss, *Phys. Rev. Lett.* **1973**, *30*, 784; b) L. A. King, W. J. Zhao, M. Chhowalla, D. J. Riley, G. Eda, *J. Mater. Chem. A* **2013**, *1*, 8935.
[20] R. Coehoorn, C. Haas, J. Dijkstra, C. J. F. Flipse, R. A. de Groot, A. Wold, *Phys. Rev. B* **1987**, *35*, 6195.
[21] X. S. Wang, H. B. Feng, Y. M. Wu, L. Y. Jiao, *J. Am. Chem. Soc.* **2013**, *135*, 5304.

© 2015 WILEY-VCH Verlag GmbH & Co. KGaA, Weinheim

[22] Y. C. Lin, W. J. Zhang, J. K. Huang, K. K. Liu, Y. H. Lee, C. T. Liang, C. W. Chu, L. J. Li, *Nanoscale* **2012**, *4*, 6637.
[23] S. Davis, J. Carver, *Appl. Surf. Sci.* **1984**, *20*, 193.
[24] L. Van der Pauw, *Philips Tech. Rev.* **1958**, *20*, 220.
[25] D. J. Late, Y.-K. Huang, B. Liu, J. Acharya, S. N. Shirodkar, J. Luo, A. Yan, D. Charles, U. V. Waghmare, V. P. Dravid, *ACS Nano* **2013**, *7*, 4879.
[26] C. C. Tsai, J. C. Knights, G. Chang, B. Wacker, *J. Appl. Phys.* **1986**, *59*, 2998.
[27] M. Fukawa, S. Suzuki, L. H. Guo, M. Kondo, A. Matsuda, *Sol. Energy Mater. Sol. Cells* **2001**, *66*, 217.
[28] S. Takanori, W. Naoya, I. Akihiro, H. Takao, A. Tanemasa, *Jpn. J. Appl. Phys.* **2011**, *50*, 06GM05.

© 2015 WILEY-VCH Verlag GmbH & Co. KGaA, Weinheim